

Optical dispersion characterization of CZTS thin films prepared by sol gel at different annealing temperature

Ali Ismail Salih

Department of Physics, College of Sciences, Kirkuk University, Kirkuk, Iraq

<https://doi.org/10.25130/tjps.v24i7.461>

ARTICLE INFO.

Article history:

-Received: 12 / 12 / 2017

-Accepted: 11 / 1 / 2018

-Available online: / / 2019

Keywords: CZTS, Sol-gel; Dispersion energy; Dispersion index; abnormal dispersion; Wemple and DiDomenico model; Burstein–Moss effect.

PACS Numbers: 78.20.-e; 78.20.ci.

Corresponding Author:

Name: Ali Ismail Salih

E-mail: aliismailsalih@gmail.com

Tel:

ABSTRACT

Thin films of (CZTS) were prepared by the sol–gel method and annealed at a range of temperatures (500, 550, 600, 650°C) under ambient condition. X-ray diffraction chart shows a preferential direction along (112) which was an indicating to the Kesterite structure. The optical properties of annealing thin films were examined by UV-Vis spectroscopy, and the energy gap was determined by the Tauc method. The band gap values increase with increasing the annealing temperature. The dispersion of refractive index of the thin film was analyzed by using the concept of single oscillator in Wemple-DiDomenico model. The average values of the dispersion energy (E_d) and the oscillator energy (E_o) of the interband optical transition were obtained, $E_d \approx 23\text{eV}$, $E_o \approx 3.775\text{eV}$ and $E_g \approx 2.15\text{eV}$. The average value of the oscillator energy has a close value to that of the energy gap, for this work $E_o \approx 1.737E_g$. It has been concluded that, as the annealing temperature of the CZTS thin films increase the optical transmittance and the energy band gap will be decreased, also there is a blue shift in the shortest optical wavelength of CZTS thin films λ_{CZTS} , from 605 to 475nm with increasing annealing temperature from 500 to 600°C.

1. Introduction

The growing need for clean renewable energy pay about the vast amount of studies in the photovoltaic devices, which are designed and fabricated mainly to harvest all possible photons, and create a useful electrical power output [1], for this results a great attention has been focused on photovoltaic thin film chalcogenides due to high energy conversion efficiency [2]. In the beginning a solar cell thin films device research focused on a polycrystalline thin films based on cadmium telluride (CdTe), copper indium selenide (CIS), and copper indium gallium selenide (CIGS) have attracted considerable interests in the past few decades. the limitations are obvious due to Rarity in In, Ga and Te and related environmental issues with the toxicity of Cd and Se, to solve these issues, it was necessary to search on a nontoxic, cheap, widespread elements and light absorber such as $\text{Cu}_2(\text{Zn},\text{Sn})(\text{S},\text{Se})_4$, which contains more widespread elements appears to have suitable photovoltaic properties [3]. The $\text{Cu}_2\text{ZnSnS}_4$ (CZTS) quaternary p-type semiconductors. has a direct band gap energy, high absorption coefficient of $>10^4\text{ cm}^{-1}$, and is environmentally friendly, non-toxic materials [4]. The band-gap energy (E_g) of CZTS, for example

(1.27eV) [5] to (2.5 eV)[6]. The reason for the E_g discrepancies was due to the complex combination of various sample preparation methods, E_g measuring means and the existence of secondary phases in the films [7].

Several methods have been used for growth CZTS p-type absorber layer, including; sol-gel spin-coated deposition [2,3,6,8,9], sol-gel dip-coating deposition [10], electro-deposition (co-electroplating) [4,5], thermal evaporation [11], magnetron sputtering, co-evaporation, hybrid sputtering, pulsed laser deposition, electron-beam evaporation, screen printing, spray pyrolysis and chemical vapor deposition [4]. Sol-Gel method is a low-cost, simple method based on hydrolysis and poly condensation reactions, often carried out by spin coating or dip coating method. The oxides are obtained by drying and annealing the coating layer in the air without vacuum system required [8], the sol is a dispersion of the solid particles with a diameter ($\approx 0.1\text{-}1\ \mu\text{m}$) in a liquid where only the Brownian motions suspend the particles and a gel is a state where both liquid and solid are dispersed in each other, which presents a solid network containing liquid components [12].

The sol-gel coating process usually consists of four steps:

- 1) The desired colloidal particles once dispersed in a liquid to form a sol.
- 2) The deposition of sol solution produces the coatings on the substrates by spraying, dipping or spinning ... etc.
- 3) The particles in sol are polymerized through the removal of the stabilizing components and produce a gel in a state of a continuous network.
- 4) Final heat treatments the remaining organic or inorganic components and form an amorphous or crystalline coating [13].

In present work, we have investigated the optical parameters were determined according to Wemple-DiDomenico model. The accurate determination of the optical constants is important, to learn the mechanisms of these phenomena to exploit and develop the interesting technological applications. Therefore, optical parameters, such as optical dispersion energies, E_o and E_d . The average values of them have been evaluated under the effect of annealing temperature.

2. Experimental Methods

CZTS precursor solution was prepared by using 2-methoxyethanol (50mL) as solvent, copper(II) acetate monohydrate (0.5M), zinc(II) acetate dihydrate

(0.25M), tin(II) chloride dihydrate (0.25M), thiourea (2M), and diethanolamine (5mL). The solid compounds of the precursors were dissolved in 2-methoxyethanol and they were stirred at room temperature for 1 h to dissolve metal compounds. DEA was added slowly drop by drop to the precursors as stabilizer. At last, the precursor was filtered and sealed. Soda-lime-glass (76.2×25.4×1 mm) used as a substrate for coating thin films, which were previously cleaned by acetone and ethanol with ultrasonic cleaning for 20 minute. Finally, all samples dried with special paper at room temperature. Sol-gel solution was deposited on glass substrate inside a spin coater chamber with 3000 r.p.s for 30 sec. By using a hot plate the layer was dried at 200°C for 10 min to evaporate the solvent and remove organic residuals. This operation was repeated to have a suitable thickness of the film. Then the films were finally annealing at temperatures (500, 550, 600 and 650°C) by using an electric furnace for 2h, figure (1) shows the experimental procedure of thin films preparation. The X-ray diffraction patterns for the prepared films were obtained using (Shimadzu XRD-6000) goniometer of copper target (1.5406 Å). The optical properties of the investigated thin film samples were measured in a wave length range of 380-1100nm, by using (UV- 1800 UV/vis Spectrophotometer).

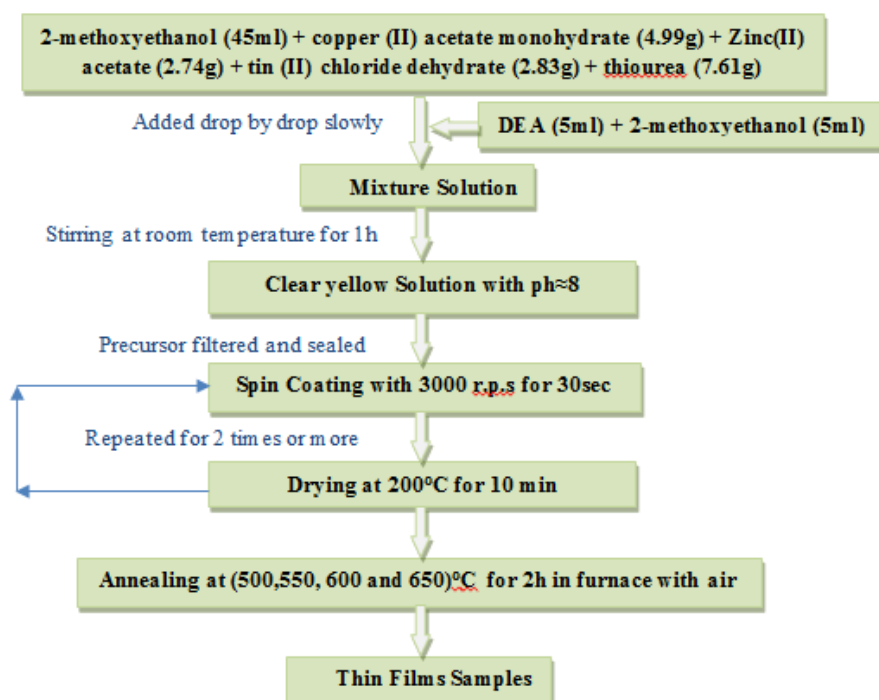


Figure 1 Experiential procedure flow chart.

3. Results and discussion

3.1 Structure properties of CZTS thin films:

The results of the x-ray tests as shown in figure (2), the XRD patterns of CZTS thin films with a broad peak were obtained at the 2θ positions 28.7°, 33.8°, 47.3° and 56.1° for the annealed films which corresponds to the tetragonal type kesterite structure of $\text{Cu}_2\text{ZnSnS}_4$ according to the JCPDS card no. 26-

0575, [6]. Extra Secondary phases were observed at high annealing temperatures 600°C and 650°C. In order to get a pure CZTS phases we suggest that the temperature does not exceed 550°C. The XRD chart shows a preferential direction along (112) which is important proves of Kesterite structure.

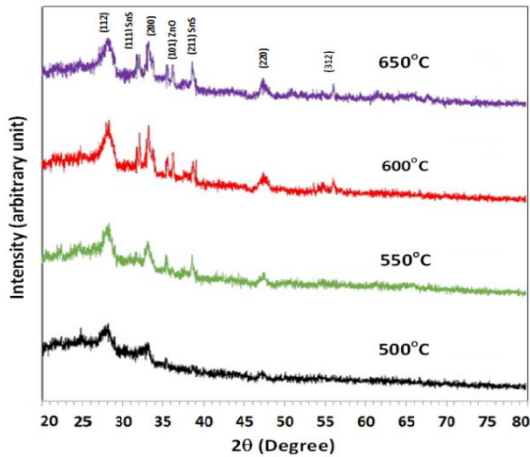


Figure 2 XRD diffraction patterns of CZTS films prepared by sol gel spin coating method at different annealing temperature.

3.2 Optical properties of spin coated CZTS thin films:

3.2.1 Transmittance:

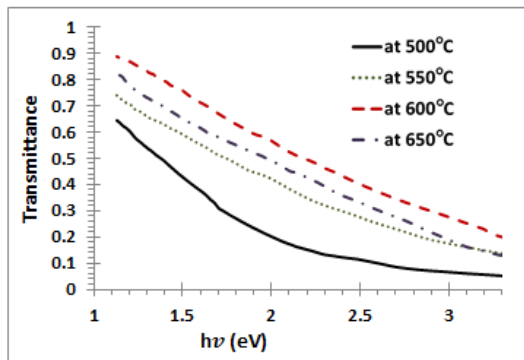


Figure 3 Transmittance vs. photon energy of CZTS thin films.

The optical transmittance spectra in Vis- NIR region of CZTS thin films annealed at different temperatures is shown in the Figure (3), we can be seen that the transmission curve increases with increasing an annealing temperature but decreases with increasing in photon energy. In region of high photon energies ($h\nu > 1.7\text{eV}$) the absorbance increases, which means that $h\nu \geq E_g$ and electrons rise from valence to conduction band. When CZTS thin films were annealed, the average transmittance was increased with increase in the annealing temperature, the absorption was shifted to the shorter wavelength, it is indicated that the carrier concentration of the thin film was increased after annealing. As a result of the annealing process, the optical band gap and the carrier concentration were increased. The increase of carrier concentration by annealing was explained by the generation of oxygen vacancies and interstitial metals due to thermal energy. The increase of the optical band gap as shown in table (3) was explained by Burstein–Moss effect due to the increased carrier concentration [14].

3.2.2 Refractive index analysis:

CZTS thin film are composed of particles which consist of; bound, conduction electrons, ionic cores,

impurities, etc. these particles moves differently with oscillating electric fields, giving rise to polarization effect at visible and infrared light frequencies, the only contribution to polarization comes from the displacement of the electron cloud, which produces an induced dipole moment, around the resonance frequency many of the optical properties of materials can be understands in terms of damped harmonic oscillator, the electrons are bounded to their cores by harmonic forces, in the presence of an external field ($-eE \exp(-i\omega t)$), their motion is given by:

$$m \frac{\partial^2 r}{\partial t^2} + m\gamma \frac{\partial r}{\partial t} + m\omega_0^2 r = -eE \exp(-i\omega t) \dots\dots\dots(1)$$

Where m and e are the mass and the charge of the electron respectively, ω_0 is the natural frequency of the oscillator, γ is a damping term and r is the electron displacement.

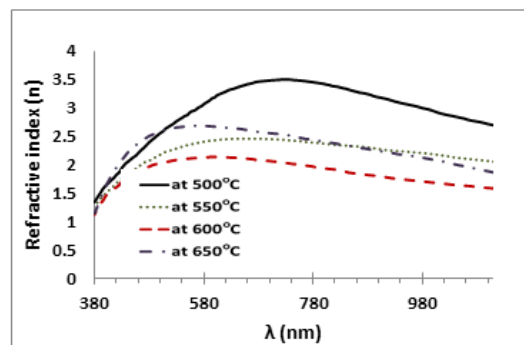


Figure 4 refractive index versus incident photon wavelength.

When the electromagnetic waves is traveling through the materials its phase velocity ($\frac{\omega}{k} = \frac{c}{n}$) where c is the speed of light in vacuum and n is the index of refraction, the refractive index curve for CZTS thin films with different annealing temperatures is shown in figure(4). These curves represent abnormal dispersion curve, for which the following important facts are to be noted:

- 1) The index of refraction increases as the wavelength decrease till (λ_{nmax}) then the refractive index decrease as the wavelength decrease.
- 2) The rate of increasing has three value ($dn/d\lambda > 0$ at shorter wave length, $dn/d\lambda < 0$ at longer wave length and $dn/d\lambda = 0$ at (λ_{nmax}).
- 3) The curve of each film depend on the annealing temperature. When the thin film has a high index of refraction, the dispersion ($dn/d\lambda$) will be change greater on both ends of (λ_{nmax}).

By analyzing the refractive index of figure (4) an important information and data can be listed in table (1).

The refractive index of CZTS is depend on the wavelength and the temperature. The $(\Delta n/\Delta T)$ is called the temperature coefficient of refractive index. When the temperature of annealing was change it will work on the occurrence of the phase transformation, the new phase will have new properties, especially it will work to get a change in the specific volume and polarizability. In order to explain the thermal change

in the refractive index of CZTS considers two counter acting effects:

- a) The growth of the specific volume is accompanied by a drop in the refractive index and vice versa.
- b) An increase in the polarizability is accompanied by a rise in the refractive index and vice versa.

The effect of these two phenomena upon the index of refraction can be derived from the relationship [15].

$$n^2 = \frac{M_v + 2R}{M_v - R} \dots\dots\dots(2)$$

Where, R stands for specific refraction and M_v for molar volume.

Table 1 the effect of annealing temperature on the some parameter which taken from refractive index curves.

T (°C)	λ_{nmax} (nm)	n_{max}	ΔT (°C)	$\Delta \lambda_{nmax}$ (nm)	Δn_{max}	$(\frac{\Delta \lambda_{nmax}}{\Delta T})$ (nm/°C)	$(\frac{\Delta n_{max}}{\Delta T})$ (1/°C)	$(\frac{\Delta n_{max}}{\Delta \lambda_{nmax}})$ (1/nm)
500	727.5	3.5	-	-	-	-	-	-
550	660	2.46	50	-67.5	-1.04	-1.35	-0.0208	0.0154
600	605	2.14	50	-55	-0.32	-1.1	-0.0064	0.0058
650	572.5	2.69	50	-32.5	0.55	-0.65	0.011	-0.0169

3.2.3 Dispersion index:

It is well known to those how have studied elementary physics that refraction causes a separation of white light into its colors. The ratio of refractive index of these two quantities in eq. (3) varies greatly for different kind of material and it is an important to characterization the dispersion of the materials, this ratio is called a dispersion index (v_D) which can be taken from refractive index curve, the dispersion index or (Abbe number) is defined as [16]:

$$v_D = \frac{n_D - 1}{n_F - n_C} \dots\dots\dots(3)$$

The difference ($n_F - n_C$) is called the principal dispersion. n_F , n_C and n_D are the refractive indices values at the 486.13 nm, 656.27 nm and 589.2 nm wavelength respectively [16]. Their values listed in table (2) for CZTS thin films. The dispersion index of CZTS thin films annealed at different annealing temperatures is shown in figure (5), the value of the absolute dispersion index has increased by increasing the annealing temperature.

Table 2 dispersion index v_D of CZTS thin films.

Annealing temperature	n_C	n_D	n_F	v_D
500°C	3.405	3.125	2.425	-2.168
550°C	2.46	2.41	2.11	-4.028
600°C	2.11	2.135	2	-10.318
650°C	2.63	2.685	2.53	-16.85

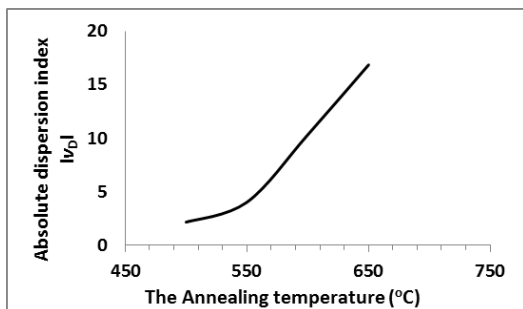


Figure 5 Absolute value of the dispersion index vs. annealing temperature

The thermal change in the refractive index and its coefficient ($\frac{dn}{dT}$) will depend upon the differences between the values of the thermal change in polarizability (ϕ), and the volume expansion (β). If $\beta > \phi$, the refractive index of optical material decreases. When $\beta \approx \phi$, the curve of the thermal dependence, β and ϕ , intersect so the coefficient ($\frac{dn}{dT}$) is either positive or negative. If $\beta < \phi$, the refractive index of CZTS increases continually [15].

3.2.4 Dispersion energy and single oscillator energy:

The dispersion of the refractive index of optical material can be analyzed by using the single oscillator model proposed by Wemple and DiDomenico. They introduced two parameters, the dispersion energy E_d which has a meaning of the oscillator strength of the interband transition which describes the dispersion of the refractive index, and the single oscillator energy E_o which has a meaning of the average interband transition energy [17].

$$n^2 - 1 = \frac{E_d E_o}{E_o^2 - (h\nu)^2} \dots\dots\dots(4)$$

By using the dispersion curves in figure (6), the values of E_o and E_d can be obtained, first, from the slope and second, from the intercept of the plot ($n^2 - 1$) versus $(h\nu)^2$. The slope of the curve was taken for the critical point at the peak value λ_{nmax} where $(dn/d\lambda) = 0$ and $E_o^2 = (h\nu)^2$. The intercept of the line at vertical axis gives (E_d/E_o).

From the observation of the average values in Table (3) we find that there is a simple experimental relationship between the single oscillator energy (E_o) and the optical band gap energy (E_g) in close approximation, ($E_o \approx 1.737 E_g$).

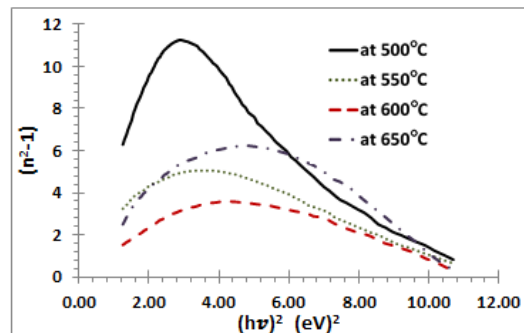


Figure 6 $(n^2 - 1)$ vs. photon energy squared.

Table 3 annealing temperature of CZTS films with dispersion energy and single oscillator energy.

Annealing temperature(°C)	E _g (eV)	E _o (eV)	E _d (eV)	E _o /E _g	E _d /E _g	E _d /E _o
500	1.8	2.57	29.298	1.428	16.277	11.4
550	2.1	3.6	18.108	1.714	8.6229	5.03
600	2.4	4.23	15.3126	1.763	6.3803	3.62
650	2.3	4.7	29.61	2.043	12.874	6.3
Average value	2.15	3.775	23.08215	1.737	11.038	6.588

As shown in table (3), E_g decrease with increasing in the annealing temperature, at 500°C CZTS thin film has lowest value E_g =1.8ev compared with thin film at 600°C where E_g =2.4 ev. that means CZTS thin film has low carriers concentration at high annealing temperature.

3.2.5 Optical wavelength inside CZTS films (λ_{CZTS}):

As the frequency of the light approaches the natural frequency, the response of the particles will be greater and large amplitude will be built up by resonance, exactly with a light with a wave length equal to λ_{CZTS}, these vibrations will in turn react upon the light wave and alter its velocity. The relation between refractive index and wave length was given by Cauchy equation[16]:

$$n^2 - 1 = \frac{A}{(1 - \frac{\lambda_0^2}{\lambda^2})} \dots\dots\dots(5)$$

Where A is constant and λ_o is the wavelength in vacuum. The velocity of the passage of the ray of light through CZTS depend upon the mutual interaction of the electric field of the ray and the outer shell electrons. The anions are more polarizable than the cations, the anions can be arranged in a sequence ordered according to the degree of their polarizability [15].

$$OH^- < O^{2-} < S^{2-} < Se^{2-}$$

The annealing temperature has an effect on the concentration of anion, a thin film of high polarizability will have a high refractive index, thus the velocity of the ray will be reduced.

$$v_\lambda = c/n_\lambda \dots\dots\dots(6)$$

Figure (7) shows the optical wavelength inside CZTS films (λ_{CZTS} = λ/n_λ), at different annealing temperature, as seen from the figure and from the table (4) there is a blue shift in the short λ_{CZTS} with increasing in the annealing temperature. The scattering of light and the color of the scattered light depends upon the size of the particles. Smaller particles scatter the light of shorter wavelength, like blue and violet and larger particles scatter longer wavelength like, red and orange.

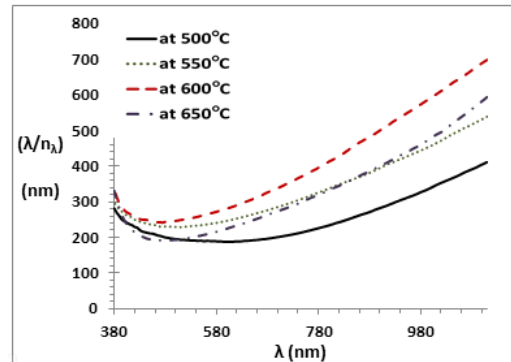


Figure 7 Optical wavelength inside CZTS films vs. incident wavelength.

Table 4 Shortest optical wavelength and their energy with different annealing temperature.

Annealing temp.(°C)	Shortest optical wavelength in CZTS films	
	λ _{CZTS} (nm)	E _{CZTS} (eV)
500	605	2.054
550	495	2.511
600	475	2.616
650	480	2.589

4. Conclusion

The CZTS thin films has been successfully deposited by sol-gel spin coating method. The X-ray diffraction pattern indicate the formation of the tetragonal type kesterite structure of CZTS thin films. The X-ray diffraction pattern shows the existing of the secondary phase in the films, it increased in their quantity of with the increasing in the annealing temperatures. Spin coated CZTS thin films are with preferred oriented (112), indicating kesterite structure. The band gap values are decreased with decreasing in the annealing temperature due to the decreasing of carrier concentration of the thin film. The band gap of the film annealed at 500°C shows a lower value 1.8 eV in present work, it is useful to use it as an absorber layer of solar cell. The refractive index values varied with annealing temperature, the maximum value was changed from 2.14 to 3.5 in the visible region, the higher was occur at a low temperature 500°C with λ=727.5nm. CZTS dispersion behavior was abnormal, the dispersion energy plays an important role in EM radiation materials interaction and in the design of spectral dispersion devices, The dispersion of the refractive index is discussed in terms of the single oscillator model.

Acknowledgement

I would like to thank all the staff in the physics department, college of science, Kirkuk university,

especially Professor Ali H. Taqi and Assistant Professor Abdel Hadi M. Galib for their constant encouragement and assistance.

References

- [1] Aristizábal, A.J. Mika, M.A. (2016) Optical Properties of CDS Films by Analysis of Spectral Transmittance. *IOSR Journal of Applied Physics*, **8(4)**: 24-31.
- [2] Li, J. et al. (2016). Optoelectronic investigation of Cu₂ZnSn(S,Se)₄ thin-films. *Science China Chemistry*, **59 (2)**: 231-236.
- [3] Guo, B. L. Chen, Y. H. Liu, X. J. Liu, W. C. and Li, A. D. (2014). Optical and electrical properties study of sol-gel derived Cu₂ZnSnS₄ thin films for solar. *AIP Advances*, **4**: 097115-10.
- [4] Mkawi, E.M., Ibrahim, K. M. Ali, K. M. and Mohamed, A. S. (2013). Dependence of Copper Concentration on the Properties of Cu₂ZnSnS₄ Thin Films Prepared by Electrochemical Method. *Int. J. Electrochem. Sci.*, **8**: 359-363.
- [5] Kanuru, C. S. Shekar, G.L. Krishnamurthy, L. Urs, R. G. K. (2014). Surface Morphological Studies of Solar Absorber Layer Cu₂ZnSnS₄ (CZTS) Thin Films by Non-vacuum Deposition Methods. *Journal Of Nano- And Electronic Physics*, **6 (2)**: 02004-10.
- [6] Chung, C. Rhee, D. Yoo, D. Choi, M. S. Heo, C. Kim, D. and Choi, C. (2013). Properties of kesterite Cu₂ZnSnS₄ (CZTS) thin films prepared by sol-gel method using two types of solution. *Journal of Ceramic Processing Research*, **14 (2)**: 255-259.
- [7] Ahn, S. et al. (2010). Determination of band gap energy (E_g) of Cu₂ZnSnSe₄ thin films: On the discrepancies of reported band gap values. *Applied Physics Letters*, **97**: 021905-3.
- [8] Tanaka, K. Moritake, N. Uchiki, H. (2007). Preparation of Cu₂ZnSnS₄ thin films by sulfurizing sol-gel deposited precursors. *Solar Energy Materials & Solar Cells*, **91**: 1199-1201.
- [9] Redha, F. W. Munef, R. A. and Salih, A. I. (2017). Effect of Concentration on Structure and morphological Properties of CZTS Thin Films Synthesized by Sol-Gel Spin Coating method. *International Journal of Recent Research and Applied Studies (IJRRAS)*, **4(10)**: 50-55.
- [10] Rajesh, G. Muthukumarasamy, N. Subramaniam, E. P. , Agilan, S. Velauthapillai, D. (2013). Synthesis of Cu₂ZnSnS₄ thin films by dip -coating method without sulphurization. *J Sol-Gel Sci Technol*, **66 (2)**: 288-293.
- [11] Ben Rabeh, M. Touatti, R. Kanzari, M. (2013). Substrate Temperature Effects on Structural Optical and Electrical Properties of Vacuum Evaporated Cu₂ZnSnS₄ Thin Films. *International Journal of Engineering Practical Research (IJEPR)*, **2 (2)**: 71-76.
- [12] Brinker, C. J. and Sherer, G. W. (1990). Sol-Gel Science: The Physics and Chemistry of Sol-Gel Processing, 1st edn., Boston: Academic press, inc.: 155pp.
- [13] Troczynski, T. and Yang, Q. (2001). Process for Making Chemically Bonded Sol-Gel Ceramics. USA, patent No. 6,284,682, May.
- [14] Chang E. K., et al. (2010). effect of carrier concentration on optical band gap shift in ZnO:Ga thin films. *Thin solid film*, **518**: 6304-6307.
- [15] Fanderlik, I. (1983). Optical properties of glass. 1st edn. Amsterda: Elsevier, 78pp.
- [16] Jenkins, F. A. White, H. E. (2001) Fundamentals of Optics. 4th edn. New york: Mc Graw-Hill, 19pp.
- [17] Alwan, T. J. (2010). Refractive Index dispersion and optical properties of dye doped polystyrene films. *Malaysian Polymer Journal*, **5 (2)**: 204-213.

دراسة خصائص التشتت البصري لأغشية CZTS الرقيقة المحضرة بطريقة السول جل عند درجات حرارة تليدين مختلفة

علي اسماعيل صالح

قسم الفيزياء ، كلية العلوم ، جامعة كركوك ، كركوك ، العراق

الملخص

حضرت اغشية (CZTS) الرقيقة بطريقة السول جل ثم لدنت على مدى من درجات الحرارة (500, 550, 600, 650°C) تحت الظروف المحيطة. وقد اظهرت مخططات الحيود للأشعة السينية بان الاتجاه المفضل للنمو كان مع المستوي (112) وهو ما أثبت ان البناء البلوري هو من نوع الكسترايت. وكذلك اجري الفحص البصري للطيف المرئي والفوق البنفسجي للأغشية الملدنة وذلك لتحديد فجوة الطاقة بطريقة (Tauc) ، ومن خلالها لوحظ بان فجوة الطاقة تزداد مع زيادة درجة حرارة التليدين. كذلك تم تحليل التشتت في معامل الانكسار للأغشية الرقيقة باستخدام مفهوم المهتر الاحادي وكما في نموذج (Wemple-DiDomenico). أما بالنسبة لمتوسط قيمة طاقة التشتت (E_d) وطاقة المهتر (E_0) للانتقالات البصرية فقد كانت القيمة كالتالي ($E_d \approx 23\text{eV}$) و ($E_0 = 3.775\text{eV}$)، وكانت ($E_g = 2.15\text{eV}$). لوحظ ان طاقة المهتر هي ذات قيمة قريبة من قيمة فجوة الطاقة وتساوي ($E_0 \approx 1.737E_g$). كذلك يمكن ملاحظة بأنه عند زيادة حرارة التليدين لمادة (CZTS) فان النفاذية البصرية وطاقة فجوة الطاقة تنخفضان. وهناك ازاحة نحو الاطوال الموجية القصيرة λ_{CZTS} من (605nm) الى (475nm) مع زيادة درجة الحرارة من (500) الى (600°C).